Nova Biotechnol Chim (2020) 19(2): 154-164
DOI: 10.36547/nbc.v19i2.737

Nova Biotechnologica *et* Chimica

Chemical bonding of polycaprolactone on the surface of hydroxyapatite via silanization and ring opening polymerization

Nadir Slimani[1,✉], Giovanni Dal Poggetto[2], Paola Laurienzo[2], Dalila Ksouri[1] and Hafit Khireddine[1]

[1] *Laboratoire de Génie de l'Environnement, Faculté de Technologie, Département de Génie des Procédés, Université de Bejaia, Bejaia 06000, Algérie*

[2] *Institute for Polymers, Composites and Biomaterials (IPCB), CNR, Via Campi Flegrei 34, Pozzuoli 80078 (Napoli), Italy*

Article info

Article history:
Received: 7th September 2020
Accepted: 7th November 2020

Keywords:
Composites
Grafting of PCL
Hydroxyapatite
ROP
Silanization
Surface modification

Abstract

In this study, surface modification of hydroxyapatite (HAp) by grafting polycaprolactone (PCL) is described. This method is carried out into two steps: (1) A treatment of HAp powder with a mixture of tetraorthosilicate (TEOS) and 3-aminopropyletriethoxysilane (APTES) to introduce amine groups and enhance nucleophilicity of surface functionalities; (2) Initiation of the Ring Opening Polymerization (ROP) of the *ε*-caprolactone (CL) in the presence of the silanized HAp. Moreover, the impact of the reaction time (24, 48 and 72 h) on the grafting amount of PCL is performed. The results of FTIR analysis confirmed the presence of carbonyl groups on the silanized HAp, providing evidence of grafting of PCL on the HAp surface. WAXS pattern showed no formation of a secondary phase after surface modification and the crystallinity is preserved. SEM/TEM analysis revealed a homogenous surface powder composed of irregular nanoscale crystals. TGA analysis indicated the dependence of PCL graft amount on the reaction time. Finally, the effect of surface modification on HAp/PCL nanocomposites morphology was investigated.

Introduction

Hydroxyapatite ($Ca_{10}(PO_4)_6(OH)_2$) is among the bioactive materials ones that elicit a specific response at the interface in contact with living tissues (Wang 2004). Due to its similarity to inorganic part of biological bone, biocompatibility, and bioactivity, it is recommended for the use as an alternative or additive for native bone (Legeros *et al.* 2008; Daculsi *et al.* 2014) such as bone filling (Furukawa *et al.* 2000), scaffolds for tissue engineering (Deville *et al.* 2006), and drug delivery systems (Itokazu *et al.* 1998).

Nevertheless, hydroxyapatite (HAp) presents poor mechanical properties, i.e. brittleness and low elastic modulus, which restricted its use to non-load bearing applications. To overcome these limitations and to broaden its applications, an intensive research has been directed towards a combination of HAp with polymeric phases. In order to get a better interfacial bonding between HAp and the organic part, thus an enhancement on mechanical properties, different strategies were adapted. Some authors reported the use of a coupling agent such as silane coupling agent (Dupraz *et al.* 1996), polyethylene glycol (Wang *et al.* 2002), diisocyanate (Liu *et al.* 1998), dodecyl alcohol (Borum-Nicholas and Wilson 2003)

✉ *Corresponding author:* boxg.nad@gmail.com

and phosphonic acid (Pramanik *et al.* 2009). Others have been looking at the use of surface modification either of the organic phase (d'Ayala *et al.* 2009; Basile *et al.* 2015); the inorganic one (Murugan *et al.* 2003; Choi *et al.* 2006; Adamska *et al.* 2013; Yala *et al.* 2013; Kobayashi *et al.* 2015) or both the organic and inorganic phases (He *et al.* 2012; Tian *et al.* 2019). Helwig *et al.* (2001) reported the graft polymerization of lactones by ROP in the presence of HAp powder with a low efficiency of hydroxyl group to initiate the polymerization, assuming that the polylactones are ionically bounded to HAp. (Wang *et al.* 2010) have used a similar method to graft caprolactone initiated by the hydroxyl group on HAp surface. They reported a maximal grafting ratio of 6.71 % during 6 h of reaction time. Exceeding this time, the grafting ratio decreases up to 5.53 % for 24 h of reaction time. (Guerra *et al.* 2006) studied HAp annealed above 600 °C and the ability of hydroxyl groups to initiate the polymerization of ε-caprolactone in an open system at room temperature. The grafting efficiency of poly(ε-caprolactone) (PCL) was influenced by the sintering temperature; in particular, annealing at 1,100 ºC during an h produces more significant proportions of PCL bonded to HAp surface. The presence of water seems to be a limiting factor due to the production of PCL not bounded to the HAp. To increase the grafting efficiency (Lee *et al.* 2006), have employed three different surface hydroxyl functionalities of HAp: unmodified HAp, HAp modified with L-lactic acid, and HAp modified with ethylene glycol (EG). A grafting degree up to 24 %, with grafting efficiency of 47 %, was reached in the case of HAp modified by EG. Among techniques to modify surface, silanization is a method used in many cases to introduce functional groups on inorganic surfaces and was applied to graft PCL on numerous materials (Kunze *et al.* 2003; Harmata *et al.* 2014). In this study, grafting of PCL on surface of HAp was achieved by two steps route. In the first step, silanization of HAp was performed in order to enhance the nucleophilicity of surface and to fulfill, in the following step, ROP of ε-caprolactone. The influence of reaction time on PCL grafting amount was investigated. Silanized HAp and PCL-grafted HAp (PCL-g-HAp) were characterized by WAXS, infrared spectroscopy, thermogravimetric analysis, N_2 adsorption, electron microscopy (SEM and TEM). In addition, a morphological study by SEM was carried out on HAp/PCL composite films, prepared by casting solution method, in order to evidence the effect of HAp modification on dispersion and interfacial adhesion between HAp filler and PCL matrix.

Experimental

Materials

The following precursors were used in this work: PCL (CAPA^{TM} 6500, Mw = 50,000 Da) was supplied by Perstop, Sweeden. Calcium nitrate tetrahydrate ($Ca(NO_3)_2.4H_2O$), phosphorus pentoxide (P_2O_5), absolute ethanol (C_2H_5OH), tetraorthosilicate ($Si(OCH_2CH_3)_4$), 3-amino-propyletriethoxysilane ($H_2N(CH_2)_3Si(OC_2H_5)_3$, tetrahydrofuran ($C_4H_8O$), anhydrous toluene ($C_7H_8$), anhydrous methylene chloride (CH_2Cl_2), Tin(II) 2-ethylhexanoate (Sn(Oct)$_2$), Chloroform ($CHCl_3$) were supplied by Sigma-Aldrich and used as received. ε-caprolactone (CL, $C_6H_{10}O_2$) was dried using vacuum distillation and calcium hydride.

Preparation of hydroxyapatite

Synthetic hydroxyapatite powder was prepared by a sol-gel approach according to the method described by (Fathi *et al.* 2008). Briefly, ethanolic solutions of calcium nitrates ($Ca(NO_3)_2.4H_2O$) and phosphorus pentoxide (P_2O_5) were merged to achieve a Ca/P molar ratio of 1.67. After 24 h of reaction time, the obtained gel was dried, then calcined at 600 ºC during 5 h. The resulted powder was sonicated in toluene for 30 min with a 500 W tip sonicator (Sonics Vibracell, USA) at 25 % power, with a 50s/50s ON/OFF cycle, before silanization step.

Surface modification of HAp by a mixture of TEOS-APTES

TEOS was dissolved in distilled water at 3 : 1 (v/v) ratio. The pH was lowered to a value of 2 by adding a solution of HCl. The solution was stirred during one hour, then 0.5 g of HAp and APTES (APTES/TEOS ratio = 3.5 : 3 v/v) were added together with 2 mL of water. The suspension was stirred for one hour (Russo *et al.* 2014). The powder was separated with a washing-centrifugation three times (at 10^4 rpm; 10 min) with tetrahydrofurane (THF) and then dried in an oven overnight under vacuum.

Grafting of PCL on hydroxyapatite surface

HAp (2 g) was placed in a round bottomed flask with dry toluene (50 mL), then were added CL (4 g) and $Sn(Oct)_2$ (0.030 g) under nitrogen atmosphere. The reaction temperature was kept at 130 ºC during a given interval time (24, 48 and 72 h). The reaction mixture was centrifuged, then the grafted powder (PCL-*g*-HAp) was purified by a repeated washing–centrifugation at 10^4 rpm for 15 min using methylene chloride to remove ungrafted free PCL and eventual unreacted monomer. Finally, the final product was dried in a vacuum oven. Both unmodified and silanized HAp were tested.

Preparation of HAp/PCL and g-HAp/PCL composite films

Composite films were prepared using a casting solution method. PCL was dissolved in chloroform at 60 ºC (10 % w/v). Unmodified or modified HAp (3 – 6 % by wt.), previously sonicated during 50 min in 1mL of chloroform, was added to the polymer solution. The dispersion was kept under magnetic stirring during 2 min. Finally, the obtained suspension was poured in a petri dish to dry.

Techniques

Powder X-ray diffraction (XRD, model PHILIPS X pert prof, analytical, system MPD) patterns were registered employing CuK_radiation at 40 mA and 50 kV. Fourier Transform Infrared-Attenuated Total Reflectance (FTIR-ATR) spectra were obtained by a Perkin-Elmer spectrometer, model Paragon 500, provided with a ZnSe attenuated total reflectance (ATR) crystal accessory. Specimens were putted in contact with the ATR crystal and pressed with a pressure clamp positioned over the crystal/sample area to permit intimate contact between the material and the crystal. Spectra were acquired in the 4,000 – 400 cm^{-1} range, with an average of 20 scans at 2 cm^{-1} resolution. Thermogravimetric analysis (TGA) was performed on a Perkin-Elmer Pyris Diamond TG-DTA apparatus from 30 to 800 ºC under nitrogen flow (50 $mL.min^{-1}$) at 5 $ºC.min^{-1}$ heating rates. Specific surface area of HAp nanocrystals was determined by Brunauer-Emmett-Teller Analysis (BET) nitrogen gas adsorption method using a NOVA 4000e analyzer (Quantachrome Instruments, Boynton Beach, FL). Scanning Electron Microscopy (SEM) analysis was carried out on a FEI QUANTA FEG 200 (USA) operating in low vacuum mode (0.60 torr) at 30 kV acceleration voltage, to characterize the morphology of HAp powders and composites. Before analysis, samples were mounted on a metal stub by means of carbon adhesive tape and coated with a 20 nm thick gold/palladium layer with a modular high-vacuum coating system Emitech K575X. Composite films were first soaked in liquid nitrogen for one minute then fractured by means of two tweezers with a sharp movement. Cross-section cryofracture surfaces were observed. Transmission Electron Microscopy (TEM) was carried out on a FEI Tecnai G12 (LAB6 source) equipped with a FEI Eagle 4 K CCD camera (USA) operating with an acceleration voltage of 120 kV, to observe the size and shape of unmodified and modified HAp nanocrystals.

Results and Discussion

Grafting of PCL on HAp surface

Grafting polymerization of ε-CL (or other lactones) on HAp nanocrystals initiated by hydroxyl groups has been widely investigated, and attempts to introduce on surface hydroxyl groups with different nucleophilicities and steric environments have been reported, as discussed in the introduction. Here, we propose a novel strategy, consisting of two stages. Firstly, the HAp powder was treated with a TEOS-APTES mixture in order to introduce amine groups (also able to initiate CL

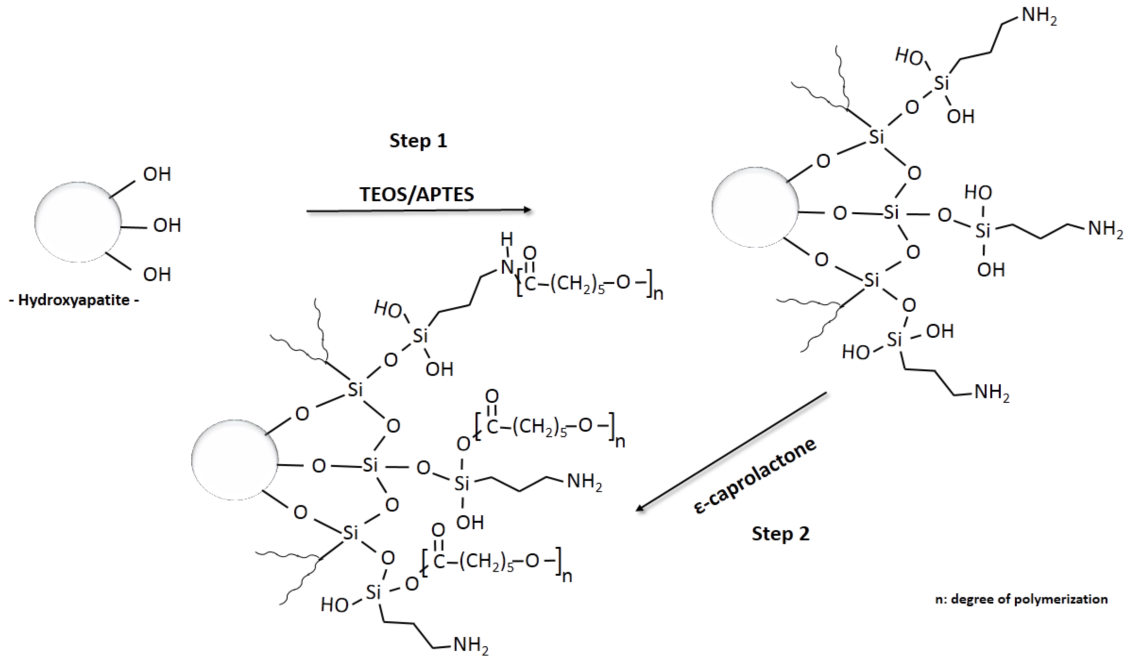

Fig. 1. Reaction scheme of the grafting method: (step 1): silanization of HAp powder, (step 2): initiation of ε-caprolactone polymerization in the presence of modified Hap; n = degree of polymerization (adapted from Russo *et al.* 2014).

polymerization) and increase the number and nucleophilicity of hydroxyl groups on the surface. In the second step, the graft polymerization of ε-caprolactone was conducted using the silanized HAp with $Sn(Oct)_2$ as a catalyst. A summarized scheme is presented in Fig. 1.

As described below, silanization of HAp surface significantly improved the anchoring efficiency of PCL chains. As a matter of fact, preliminary attempts to initiate CL polymerization using directly the surface hydroxyl groups of unmodified HAp completely failed. The low reactivity of hydroxyl groups directly linked to the surface is reasonably due to steric hindrance.

FTIR characterization

FTIR-ATR spectra of the unmodified and silanized HAp are shown in Fig. 2. The bands at 3,571 and 629 cm^{-1} belong to the respective stretching, librational and translational modes of HO^- ions (Meski *et al.* 2011). The bands of significant intensity at 1,085 and 1,023 cm^{-1} arise from ν3 vibrational mode of the PO_4^{3-} tetrahedral (Yala *et al.* 2013). The bands at 961 cm^{-1} and 563 – 599 cm^{-1} correspond to ν1 and ν4 symmetric P–O stretching vibration of the PO_4^{3-} ions, respectively (Fathi *et al.* 2008). The bands between 1,420 – 1,456 cm^{-1} correspond to the ν3 vibrational modes of carbonates. The ν2 vibrational mode of carbonate is also detected at 875 cm^{-1} (Varma and Babu 2005). The presence of carbonates is explained by a substitution of part of PO_4^{3-} ions by CO_3^{2-} ions, known as B-type carbonated HAp. Carbonate ions are probably produced by the absorption of carbon dioxide, present at the atmosphere, by the solution of ethanol. The mechanism of this reaction is as follows (Yala *et al.* 2016):

$$CO_2 + 2H_2O \leftrightarrow H_2CO_3 + H_2O$$

$$H_2CO_3 + OH^- \leftrightarrow HCO_3^- + H_2O$$

$$HCO_3^- + OH^- \leftrightarrow CO_3^{2-} + H_2O$$

The silanized powder shows additional bands; among others, the bands around 1,100 cm^{-1} belong to the asymmetric stretching of the Si-O bound of the silanol groups (Russo *et al.* 2014). The band around 1,560 cm^{-1} is attributed to the bending vibration of amine groups NH_2. The bands approximately between 2,936 – 2,865 cm^{-1} are assigned to stretching vibration of C-H. Moreover, the shallow band around 460 cm^{-1} is attributed to the scissoring absorption mode of Si-O-Si siloxane groups (Majoul *et al.* 2015). These results indicate that APTES was properly deposited

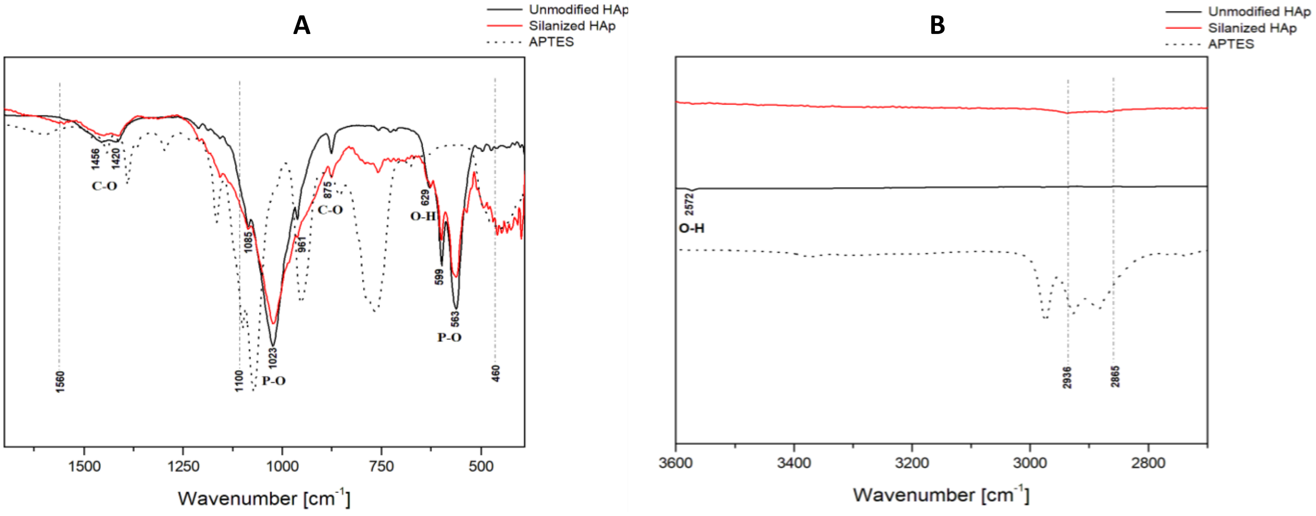

Fig. 2. FTIR spectra of unmodified HAp, silanized HAp and APTES from 400 – 1,700 cm^{-1} (**A**), from 2,700 – 3,600 cm^{-1} (**B**).

on the HAp surface. After surface polymerization with ε-caprolactone (Fig. 3), no new adsorption peaks were observed for the pure HAp, indicating that the hydroxyl groups present on the surface of pure HAp did not promote the polymerization of ε-caprolactone. Instead, the silanized HAp presents two new adsorptions bands at 1,730 cm^{-1} and 1,639 cm^{-1} belonging respectively to the stretching vibration of carbonyl groups –O-C=O of PCL (Wang *et al.* 2010) and to secondary amide deriving from grafting of PCL on $–NH_2$ functionalities. The band at 1,551 cm^{-1} is attributed to a mixed vibration of N-H bending and C-N stretching in secondary amides. The appearing of amide bands accounts for formation of PCL initiated by amine groups rather than hydroxyl groups. The increase of the intensity of amide bands after 48 h is likely due to increase of the number of polymer chains rather than growing of already existing chains. On the contrary, after 72 h the carbonyl band is more intense with respect to the amide bands, accounting for growing of the pre-existing PCL grafted chains.

Structural Characterization

WAXS pattern of the prepared nanoparticles of HAp and the modified ones are shown in the

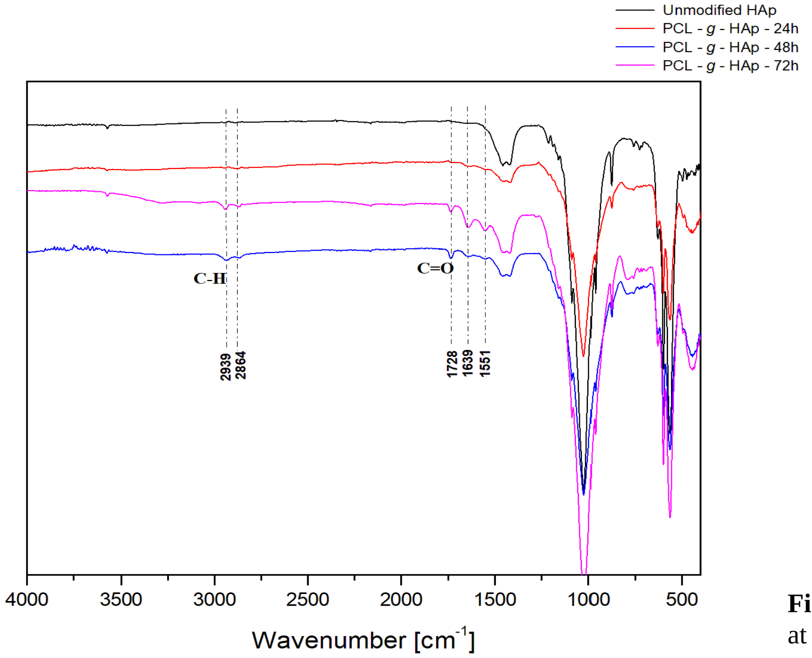

Fig. 3. FTIR spectra of HAp and PCL-g-HAp at the various reaction times.

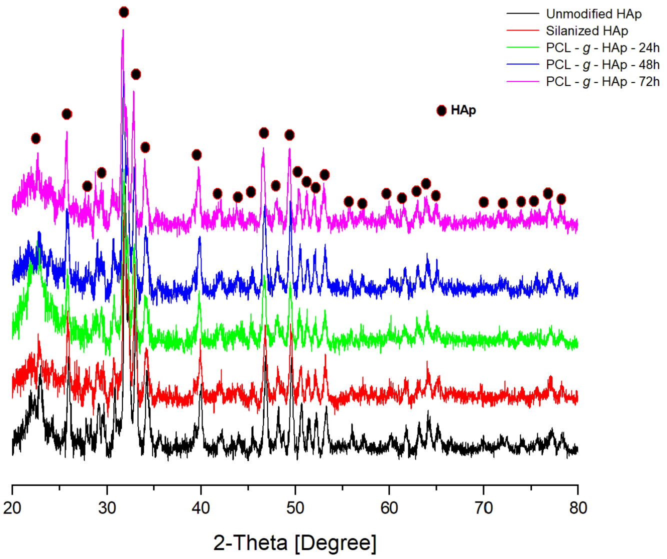

Fig. 4. WAXS pattern of the unmodified and modified HAp.

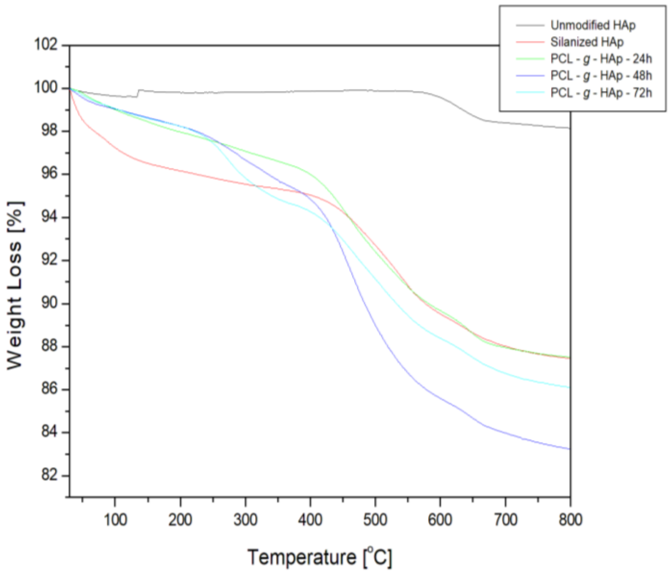

Fig. 5. TGA curves of pure and modified HAp.

Fig. 4. These latter reveal several sharp peaks at 20 regions of 26 º, 32 – 34º, 40º, and 46 – 54º that are coherent with the crystalline nature of HAp nanoparticles (Fathi *et al.* 2008). The pattern of all samples presents almost the same result. Neither position modification nor new peaks were observed after silanization or grafting with PCL. It means that the crystalline nature of HAp was preserved and no secondary phase was formed after surface modification. These results support previous studies on the grafting of PCL on the surface of HAp (Choi *et al.* 2006; Wang *et al.* 2010).

Thermogravimetric Analysis

Thermogravimetric analysis was performed to further evidence the presence of the organic polymeric phase on the modified HAp. For sake of comparison, HAp and silanized HAp were also analyzed. Three thermal events are observed (Fig. 5). The first step (up to 200 ºC) can be ascribed to the departure of the physisorbed water molecules, and is more pronounced in the case of silanized HAp, which exhibits a higher tendency to absorb water. The second one between 200 and 400 ºC is ascribed exclusively to the removal of the organic phase (PCL), since no weight loss was detected in this range for both HAp and silanized HAp. The third step between 400 and 600 ºC can be attributed to the departure of carbon chains like CO and CO_2 or to SiO groups (Douard *et al.* 2010). Finally, a small loss was observed between 600 and 00 ºC assigned to the departure of water during structural transformation (Saoiabi *et al.* 2012). The amount of PCL grafted on HAp was measured directly from the TGA curves, since it corresponds to the weight loss [%] in the range 200 – 400 ºC as reported in the Table 1. The percentage grafting and grafting efficiency was determined by Eq. 1:

$$Grafting\ efficiency\ [\%] = \frac{grafted\ PCL\ on\ HAp\ (g)}{CL\ used\ (g)} \times 100 \qquad (1)$$

As can be seen from Table 1, the amount of grafted PCL regularly increases with the reaction time. A relatively low PCL grafting ratio was obtained, with a grafting efficiency 2 %. Nevertheless, it must be noted the significant improvement with respect to unmodified HAp, which was found to be fully unable to initiate CL polymerization. Hence, the obtained results represent a general proof-of-principle that silanization of HAp is a good tool to increase the number and the reactivity of surface hydroxyl groups, and, in addition, also to introduce amine functionalities.

Table 1. Weight loss between 200 and 400 ºC (corresponding to the amount of grafted PCL) and grafting efficiency of PCL-g-Hap at the various reaction times.

Sample	Weight loss [%]	Grafting efficiency [wt. %]
PCL-g-HAp-24 h	1.968	1.00
PCL-g-HAp-48 h	3.396	1.75
PCL-g-HAp-72 h	3.952	2.00

BET analysis

Nitrogen adsorption - desorption isotherms of the unmodified HAp, PCL-g-HAp-48 h and PCL-g-HAp-72 h are shown in Fig. 6. As observed, the adsorption capacity increases when the relative pressure (P/P^o) is higher than 0.85, with a hysteresis loop in the adsorption-desorption cycle, attributed to H3 type according to IUPAC recommendation (Thommes *et al.* 2015). Adsorption-desorption results indicate the presence of micropores. The hysteresis loop is probably due to an artifact. Nitrogen adsorption-desorption revealed a specific surface area of 6.68 m^2.g^{-1} for the unmodified HAp, which is close to the value reported in literature for natural HAp (Sobczak-Kupiec *et al.* 2012). No significant variations of surface area were detected upon modification, proving that grafting of PCL on the surface did not affect the porosity of HAp.

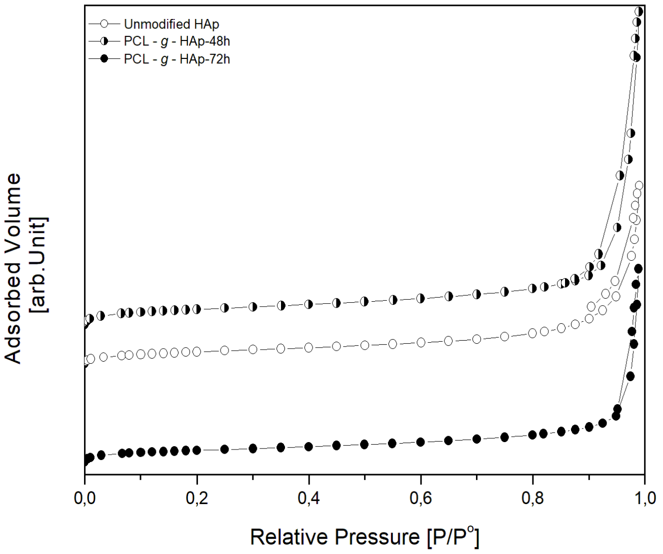

Fig. 6. Adsorption-desorption of nitrogen 77 [k] of un-modified HAp and the grafted ones.

SEM and TEM analysis

SEM analysis of HAp shows a porous powder,

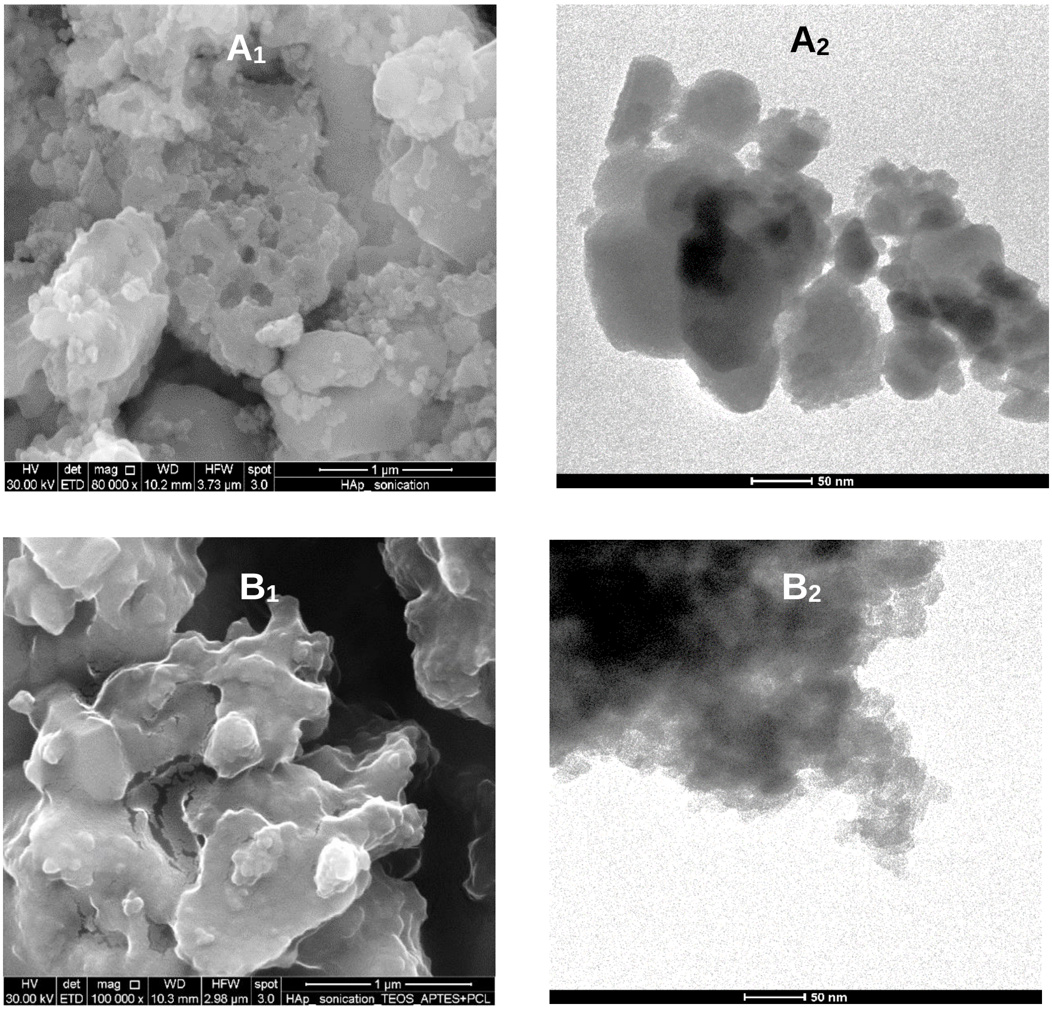

Fig. 7. SEM and TEM images of unmodified HAp (**A**$_1$, **A**$_2$) and of PCL-g-HAp-72 h (**B**$_1$, **B**$_2$).

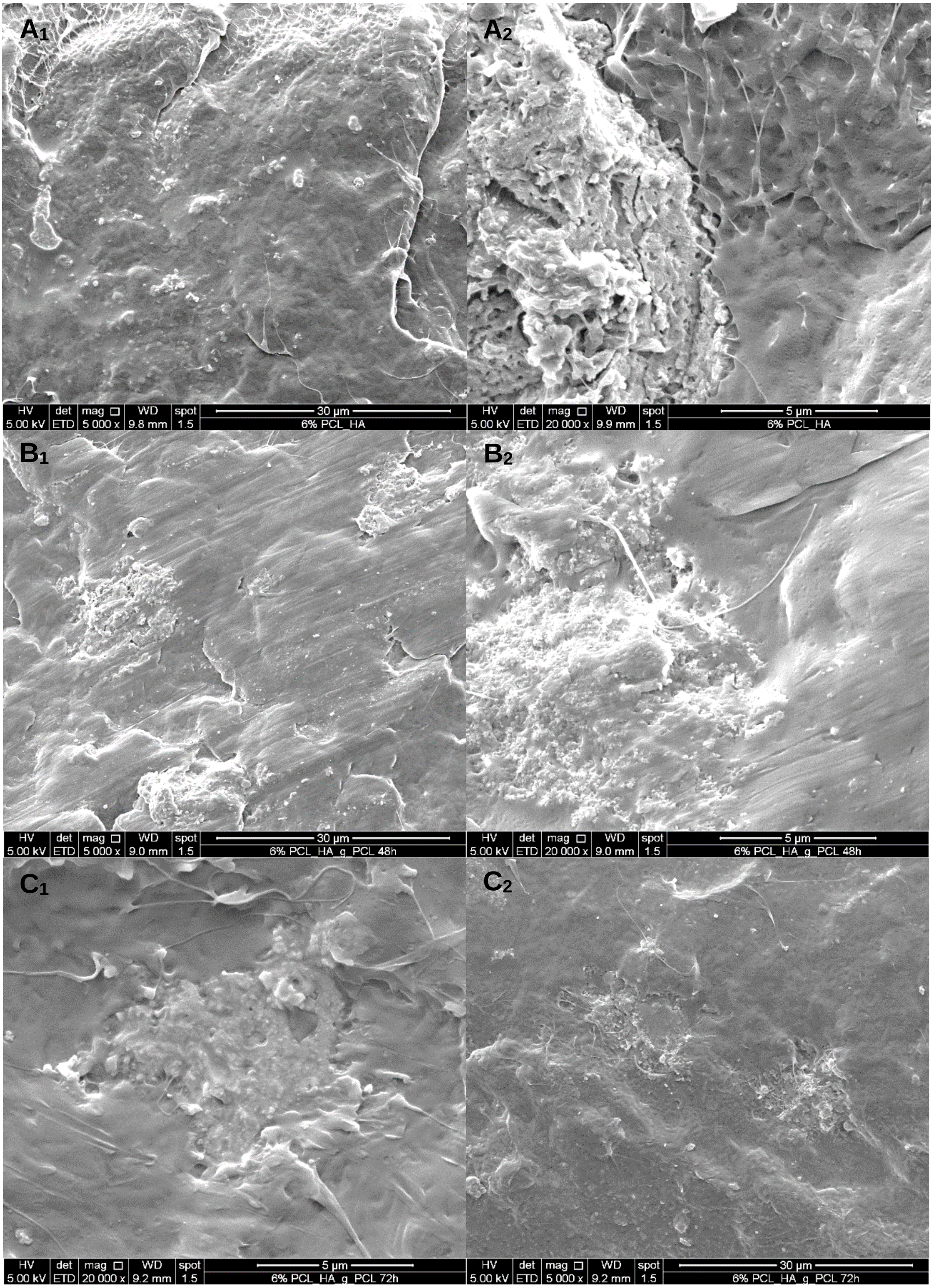

Fig. 8. Fracture surface SEM images of the composite films at different magnifications: HAp/PCL 6 % (**A**$_1$: ×5, 000; **A**$_2$**:** ×20,000), PCL-*g*-HAp-48h/PCL 6 % (**B**$_1$: ×5,000*;* **B**$_2$**:** ×20,000), PCL-*g*-HAp-72 h/PCL 6 % (**C**$_1$**:** *×5,000;* **C**$_2$**:** ×20,000).

consisting of agglomerates. A smooth, homogenous surface is observed after grafting with PCL (Fig. 7A$_1$ and 7B$_1$). This leads to assume that the polymer is homogeneously distributed, forming a coating on the surface of the inorganic phase. The pores are no more visible after grafting. TEM images shows that the HAp nanoparticles are composed of irregular crystals of about 91 nm in length and 69 nm in width (Fig. 7A$_2$ and 7B$_2$). The crystallites shape and size are not significantly influenced by PCL grafting, probably due to the low PCL content.

The next point was to verify whether the use of PCL grafted-HAp in PCL based composites can play a role in improving dispersion and interfacial adhesion. Cross sections obtained by cryo-fracture of films of HAp/PCL and PCL-*g*-HAp/PCL composites were observed by SEM. Photos showed that the samples present different fracture surface morphology, pointing out differences in agglomeration and bonding to the polymer matrix of HAp fillers. Micrographs of the different composites at 6 % HAp content are reported in Fig. 8. The HAp fillers appear to be more homogenously distributed after surface modification, and a better incorporation within the polymer matrix is noted. In particular, photos at higher magnification clearly evidence how HAp fillers are completely detached from the polymeric matrix in the case of HAp/PCL composite (Fig. 8A$_2$), whereas they are well adherent in the case of PCL-*g*-HAp/PCL composites (Fig. 8B$_2$ and 8C$_2$). This feature is more remarkable in PCL-g-HAp-72 h/PCL, as expected, due to the higher amount of grafted PCL. Moreover, HAp fillers appear really coated with polymer in both PCL-*g*-HAp/PCL composites. These results demonstrate that even a low amount of PCL covalently grafted on HAp surface is able to reduce HAp agglomeration and to keep a better interfacial adhesion. The trend is similar in the 3 % composites (photos not shown).

Conclusions

In the present work, a novel strategy to chemically graft PCL chains on HAp surface by ROP polymerization of *ε*-caprolactone is described. Preliminary results confirmed that the hydroxyl groups present on HAp surface are not effective to initiate graft polymerization of *ε*-caprolactone. Therefore, a pre-functionalization is necessary to provide reactive sites for chemically coupling the organic polymer. The silanization of HAp revealed to be an easy and essential step in this process; polycaprolactone was then successfully grafted on HAp by ring opening polymerization of CL. At our knowledge, this is the first example of combination of silanization with ROP polymerization of *ε*-caprolactone to enhance grafting of PCL on HAp surface. WAXS and FTIR-ATR analyses confirmed that the surface modification was held only at the surface since no crystalline modification was detected. Moreover, the grafting degree was proportional to the reaction time, as evidenced by TGA analysis. BET analysis evidenced a microporous texture of HAp, and no significant variations in the texture properties were found after grafting. Finally, morphological analysis by SEM of HAp/PCL and PCL-g-HAp/PCL composite films showed improved compatibility between PCL-g-HAp filler and PCL matrix, demonstrating that an amount of around **4** % by wt. of grafted PCL is enough to improve distribution and adhesion of the inorganic phase.

Acknowledgment

The authors wish to thank Dr. Rachele Castaldo and Mrs. Cristina Del Barone (IPCB) for the helpful discussion on BET analysis and the technical assistance in SEM and TEM analysis, respectively.

Conflict of Interest

The authors declare that they have no conflict of interest.

References

Adamska K, Szubert M, Voelkel A, Okulus Z (2013) Characterisation of hydroxyapatite surface modified by poly (ethylene glycol) and poly (hydroxyethyl methacrylate) grafting. Chem. Pap. 67: 429-436.

Basile MA, d'Ayala GG, Malinconico M, Laurienzo P, Coudane J, Nottelet B, Ragione FD, Oliva A (2015) Functionalized PCL/HA nanocomposites as microporous membranes for bone regeneration. Mater. Sci. Eng. C. 48: 457-468.

Borum-Nicholas L, Wilson O (2003) Surface modification of hydroxyapatite. Part I. Dodecyl alcohol. Biomaterials 24: 3671-3679.

Choi HW, Lee HJ, Kim KJ, Kim H-M, Lee SC (2006) Surface modification of hydroxyapatite nanocrystals by grafting polymers containing phosphonic acid groups. J. Colloid Interface Sci. 304: 277-281.

Daculsi G, Fellah BH, Miramond T (2014) The essential role of calcium phosphate bioceramics in bone regeneration. *In* Ben-Nissan B (Eds.), Advances in calcium phosphate biomaterials, Springer-Verlag, Berlin Heidelberg, pp. 71-96.

D'Ayala GG, Di Pace E, Laurienzo P, Pantalena D, Somma E, Nobile MR (2009) Poly (ε-caprolactone) modified by functional groups: Preparation and chemical–physical investigation. Eur. Polym. J. 45: 3217-3229.

Deville S, Saiz E, Tomsia AP (2006) Freeze casting of hydroxyapatite scaffolds for bone tissue engineering. Biomaterials 27: 5480-5489.

Douard N (2010) Élaboration et fonctionnalisation de biocéramiques phosphocalciques. Doctoral dissertation thesis, Limoges.

Dupraz AMP, vd Meer SAT, De Wijn JR, Goedemoed JH (1996) Biocompatibility screening of silane-treated hydroxyapatite powders, for use as filler in resorbable composites. J. Mater. Sci. Mater. Med. 7: 731-738.

Fathi M, Hanifi A, Mortazavi V (2008) Preparation and bioactivity evaluation of bone-like hydroxyapatite nanopowder. J. Mater. Process. Technol. 202: 536-542.

Furukawa T, Matsusue Y, Yasunaga T, Nakagawa Y, Okada Y, Shikinami Y, Okuno M, Nakamura T (2000) Histomorphometric study on high-strength hydroxyapatite/poly (l-lactide) composite rods for internal fixation of bone fractures. J. Biomed. Mater. Res. Part A. 50: 410-419.

Guerra G, Cerrai P, Tricoli M, Krajewski A, Ravaglioli A, Mazzocchi M, Barbani N (2006) Composites between hydroxyapatite and poly (ε-caprolactone) synthesized in open system at room temperature. J. Mater. Sci. Mater. Med. 17: 69-79.

Harmata AJ, Ward CL, Zienkiewicz KJ, Wenke JC, Guelcher SA (2014) Investigating the effects of surface-initiated polymerization of ε-caprolactone to bioactive glass particles on the mechanical properties of settable polymer/ceramic composites. J. Mater. Res. 29: 2398-2407.

He J, Yang X, Mao J, Xu F, Cai Q (2012) Hydroxyapatite–poly (L-lactide) nanohybrids via surface-initiated ATRP for improving bone-like apatite-formation abilities. Appl. Surf. Sci. 258: 6823-6830.

Helwig E, Sandner B, Gopp U, Vogt F, Wartewig S, Henning S (2001) Ring-opening polymerization of lactones in the presence of hydroxyapatite. Biomaterials 22: 2695-2702.

Itokazu M, Yang W, Aoki T, Ohara A, Kato N (1998) Synthesis of antibiotic-loaded interporous hydroxyapatite blocks by vacuum method and in vitro drug release testing Biomaterials 19: 817-819.

Kobayashi S, Nagao R (2015) Effect of surface modification of β-tricalcium phosphate on mechanical properties of poly (L-lactic acid) composites. Adv. Compos. Mater. 24: 467-480.

Kunze C, Freier T, Helwig E, Sandner B, Reif D, Wutzler A, Radusch HJ (2003) Surface modification of tricalcium phosphate for improvement of the interfacial compatibility with biodegradable polymers. Biomaterials 24: 967-974.

Lee HJ, Choi HW, Kim KJ, Lee SC (2006) Modification of hydroxyapatite nanosurfaces for enhanced colloidal stability and improved interfacial adhesion in nanocomposites. Chem. Mater. 18: 5111-5118.

Legeros RZ, Legeros JP (2008) Hydroxyapatite. *In* Kokubo T (Eds.), Bioceramics and their Clinical Applications, Woodhead Publishing, New York, pp. 367-394.

Liu Q, de Wijn JR, de Groot K, van Blitterswijk CA (1998) Surface modification of nano-apatite by grafting organic polymer. Biomaterials 19: 1067-1072.

Majoul N, Aouida S, Bessaïs B (2015) Progress of porous silicon APTES-functionalization by FTIR investigations. Appl. Surf. Sci. 331: 388-391.

Meski S, Ziani S, Khireddine H, Boudboub S, Zaidi S (2011) Factorial design analysis for sorption of zinc on hydroxyapatite. J. Hazard. Mater. 186: 1007-1017.

Murugan R, Rao KP (2003) Graft polymerization of glycidylmethacrylate onto coralline hydroxyapatite. J. Biomater. Sci., Polym. Ed. 14: 457-468.

Pramanik N, Mohapatra S, Bhargava P, Pramanik P (2009) Chemical synthesis and characterization of hydroxyapatite (HAp)-poly (ethylene co vinyl alcohol) (EVA) nanocomposite using a phosphonic acid coupling agent for orthopedic applications. Mater. Sci. Eng. C. 29: 228-236.

Russo L, Taraballi F, Lupo C, Poveda A, Jiménez-Barbero J, Sandri M, Tampieri A, Nicotra F, Cipolla L (2014) Carbonate hydroxyapatite functionalization: a comparative study towards (bio) molecules fixation. Interface Focus 4: 20130040.

Saoiabi S, El Asri S, Laghzizil A, Masse S, Ackerman JL (2012) Synthesis and characterization of nanoapatites organofunctionalized with aminotriphosphonate agents. J. Solid State Chem. 185: 95-100.

Sobczak-Kupiec A, Malina D, Kijkowska R, Wzorek Z (2012) Comparative study of hydroxyapatite prepared by the authors with selected commercially available ceramics. Dig. J. Nanomater. Biostructures 7: 385-391.

Thommes M, Kaneko K, Neimark AV, Olivier JP, Rodriguez-Reinoso F, Rouquerol J, Sing KSW (2015) Physisorption of gases, with special reference to the evaluation of surface area and pore size distribution (IUPAC Technical Report). Pure Appl. Chem. 87: 1051-1069.

Tian G, Zhu G, Xu S, Ren T (2019). A novel shape memory poly (ε-caprolactone) /hydroxyapatite nanoparticle networks for potential biomedical applications. J. Solid State Chem. 272: 78-86.

Varma H, Babu SS (2005) Synthesis of calcium phosphate bioceramics by citrate gel pyrolysis method. Ceram. Int. 31: 109-114.

Wang M (2004) Bioactive materials and processing. *In* Shi D (Eds.), Biomaterials and tissue engineering, Springer-

Verlag, Berlin Heidelberg, pp. 1-82.

Wang X, Li Y, Wei J, De Groot K (2002) Development of biomimetic nanohydroxyapatite/poly (hexamethylene adipamide) composites. Biomaterials 23: 4787-4791.

Wang Y, Dai J, Zhang Q, Xiao Y, Lang M (2010) Improved mechanical properties of hydroxyapatite/poly (ε-caprolactone) scaffolds by surface modification of hydroxyapatite. Appl. Surf. Sci. 256: 6107-6112.

Yala S, Boustta M, Gallet O, Hindié M, Carreiras F, Benachour H, Sidane D, Khireddine H (2016) New synthesis method of HA/P (D, L) LA composites: study of fibronectin adsorption and their effects in osteoblastic behavior for bone tissue engineering. J. Mater. Sci. Mater. Med. 27: 140.

Yala S, Khireddine H, Sidane D, Ziani S, Bir F (2013) Surface modification of natural and synthetic hydroxyapatites powders by grafting polypyrrole. J. Mater. Sci. 48: 7215-7223.